In vivo proton magnetic resonance spectroscopic signal processing for the absolute quantitation of brain metabolites

Pravat K. Mandal*

Neurospectroscopy and Neuroimaging Laboratory, National Brain Research Centre, Gurgaon, India

ABSTRACT

Magnetic resonance spectroscopy (MRS) is a non-invasive imaging modality for metabolite detection in different parts of the body (e.g. brain, liver, prostate, breast, kidney, skeletal muscle, and heart) for normal person as well as in various disorders. It aids in providing valuable information for both diagnosis as well as therapeutic monitoring. Though there has been tremendous progress in MRS signal processing techniques for the quantitation of neurometabolites, variability in the absolute quantitation of metabolites persists due to various experimental conditions. In this article, we present in-depth discussion on ^{1}H MRS data processing and quantitation using different software packages both in frequency (e.g. LCModel) and time domain (e.g. jMRUI). We have included comparative analysis of precision and accuracy of MRS data processing using LCModel and jMRUI (AMARES). Special emphasis has been provided for the handling of macromolecules and lipid in LCModel and jMRUI methods. The author also suggests certain points to be noted while opting for above software packages.

© 2011 Elsevier Ireland Ltd. All rights reserved.

1. Introduction

Nuclear magnetic resonance (NMR) is an important biophysical method for the *in vitro* determination of protein structure and protein–drug interaction studies [1–3]. Magnetic Resonance Imaging (MRI), based on the principles of NMR, is a powerful non-invasive biomedical application tool (*in vivo*) to visualize different regions of the body which provides greater image contrast between normal and abnormal tissues (e.g. tumor and cancer) for diagnostic purposes. The spectrometer, popularly known as an "MRI scanner", generates data and subsequently anatomical images are produced. The same MRI scanner is used for creating metabolite images for different parts of the body (e.g. brain, liver, prostate, breast, kidney, skeletal muscle, and heart) using magnetic resonance spectroscopy (MRS). The principal difference between these two (MRI and MRS) *in vivo* imaging modalities depends on the pulse sequences used for data generation. Magnetic resonance spectroscopic imaging (MRSI) is the combination of both spectroscopic and imaging technique to produce the distribution of metabolites within the tissue under investigation.

The task and challenge in generating good quality MRS data from various organs are different due to repeated gross or pulsatile motion leading to poor shimming and consequently increased linewidths of the metabolite peaks [4]. It is also difficult to suppress or separate the lipid peaks from metabolites of interest. Clinically, brain has poor accessibility for biopsies compared to other body organs [5] and imaging technique serves as important noninvasive diagnostic method in clinical setup. MRS studies on brain are advantageous compared to other body organs due to: (i) easier to shim the spherical shaped brain and least biologic motion of brain tissue unlike other body organs (liver, kidney, and heart) and (ii) the separation of lipid peaks from neurometabolites is well resolved in the brain.

Broadly, the experimental parameters and conditions setting for generating MRS data involve good shimming (to overcome the susceptibility effect), biological motion compensation, pulse angle calibration, appropriate time setting involving echo time (TE) and repetition time (TR) based on the relaxation times (e.g. longitudinal (T_1), transverse (T_2) or $T_2{}^*$) of various tissues under investigation. Detailed discussion on this experimental aspect is out of the purview of this manuscript.

The focus of this article is on ^{1}H MRS data processing and quantitation of brain neurometabolites. The outline of this manuscript is as follows: (i) brief description of MRS methodology as well as the clinical application of MRS; (ii) preprocessing steps and principles for quantitation of metabolites in time and frequency domains; (iii) detailed description of preprocessing of MRS data and metabolite quantitation using LCModel, and jMRUI software

* Tel.: +91 9910318922.
  E-mail address: pravat.mandal@gmail.com (Dr. Mandal).

packages; (iv) comparative analysis of data quality processed by LCModel, and jMRUI software packages and (v) handling of the macromolecules and lipids using above mentioned software packages.

1.1. Brief description of MRS methodology

In vivo ^{1}H MRS and ^{31}P MRS are the most widely used applications in MRS technique; however, MRS studies are also possible using other nuclei (e.g. ^{13}C, ^{19}F, ^{15}N, and ^{23}Na). Signals from neurometabolites consisting of different nuclei are represented either as signal amplitude in the time domain, or peak-area in the frequency domain, which is directly correlated to the concentration of the assigned metabolite displayed along the Y-axis [6]. Generally, ^{1}H and ^{31}P MRS techniques are used to detect different metabolites such as N-acetylaspartate (NAA), a neuronal marker, GPC (glycerophosphocholine) and PC (phosphocholine), important cell membrane components, Cr (creatine) and PCr (phosphocreatine), involved in energy metabolism, and mI (myo-inositol), a glial marker that is elevated in cancer cells. The most frequently used ^{1}H MRS pulse sequences are PRESS (point-resolved spectroscopy) [9] or STEAM (stimulated echo acquisition mode) [7]. Detailed mathematical description of these two pulse sequences is presented elsewhere [6]. MRS data (^{1}H, ^{31}P or ^{13}C) can be generated from ^{1}H MRS, proton decoupled ^{31}P MRS [8] and ^{13}C MRS [9] experiments. It is important to note that ^{13}C and or ^{31}P nuclei have low gyromagnetic ratios compared to protons. Hence, to attain better sensitivity for ^{31}P or ^{13}C MRS spectra, these experiments are performed by utilizing the Nuclear Overhauser effect by taking advantage of the higher gyromagnetic ratio of the proton [10]. Magnetic field strength (e.g. 1.5 T, 3 T, and 7 T) plays an important role for the quality of MRS data. 3 T scanner is now widely available and permitted for routine clinical use; however, 7 T scanner now available exclusively for research purpose and not in a clinical setting yet. The spatial resolution of MR spectra increases with magnetic field strength. At higher field MRI scanner, signal to noise ratio (SNR) of the metabolites increases approximately linearly with field strength. Hence, good quality data can be collected with reduced number of scans in higher field scanner and MRS experimental time is saved, which is crucial in a clinical setting. It is important to note that with increase in magnetic field strength, relaxation times of metabolites are influenced (e.g. longitudinal relaxation time, T_1 lengthens with field strength and transverse relaxation time, T_2 decreases with field strength and magnetic susceptibility effects increase with field strength). Hence, the proper calibration of experimental parameters (e.g. echo time, repetition time and optimized flip angle setting) is required at high magnetic field strength scanner for MRS studies [11–13].

1.2. Brief description on the clinical application of ^{1}H MRS

The analysis of different neurochemicals using ^{1}H MRS technique is extremely helpful for various brain disorders: Alzheimer [6,14,15], Parkinson [16,17], bipolar disorder [18,19], schizophrenia [20,21], etc. The ^{1}H MRS studies are also important for clinical studies outside of brain [5] involving breast tumor/cancer [22,23], liver disorder [24], prostate cancer [25] and skeletal muscle disorder [26,27].

1.3. Common terminologies often used in MRS

1.3.1. Field of view (FOV)

FOV represents the area of the brain or other parts of the body under investigation. FOV is generally expressed in specific dimensions (e.g. 210 mm, Anterior to Posterior, AP; 190 mm Right to Left, RL, slice thickness of 15 mm). In the specified FOV, selection of spa-
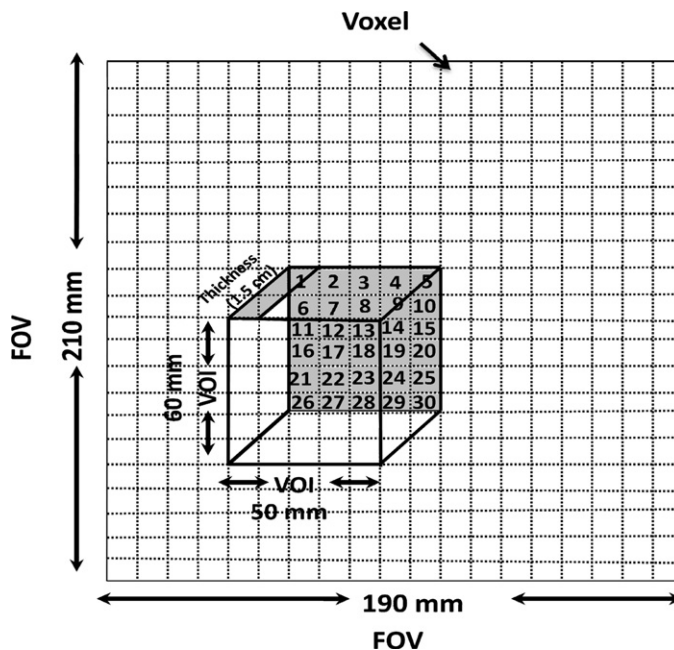
Fig. 1. Schematic representation of voxel, field of view and volume of interest. In the figure, we have 399 voxels in total, as FOV; however, only 30 voxels are in VOI. Tissue from this region is actually excited by the selective pulse and signals are analyzed. VOI is also sometimes referred to as Region of Interest (ROI).

tial resolution is accomplished with the help of phase encoding gradients. Fig. 1 shows the graphical presentation of FOV.

1.3.2. Volume of interest (VOI)

VOI refers to the actual region under investigation. In the case of single-voxel MRS, VOI is achieved with the involvement of three slice selective pulses (either three successive 90° pulses, or one 90° and two successive 180° pulses) applied in the presence of gradients. In the case of multi-voxel data collection, VOI with specific dimension (e.g. 60 mm AP, 50 mm RL) is selected within the FOV (Fig. 1). In case of smaller voxel size, longer experiment time is required to achieve reasonable signal-to-noise ratio (SNR), and SNR increases with voxel size increment due to higher tissue content as shown in the equation below.

$$\text{SNR} = C(\text{voxel size})\sqrt{\frac{\text{number of experiments performed}}{\text{spectral bandwidth}}} \qquad (1)$$

where C is a constant. In case of single voxel experiments, VOI and voxel size are same. Detailed information on multiple-voxel methodology can be found elsewhere [28,29].

1.4. Single-voxel and multiple-voxel MRS

In the single voxel MRS technique, a cubic or rectangular volume element (referred to as single-voxel) is selected with the help of slice selective pulses as well as gradients. The size of the single-voxel is generally expressed in volume (e.g. 20 mm × 20 mm × 20 mm) for a particular region of the brain. However, in multiple-voxel MRS, known as MRSI, experiments are performed covering larger regions consisting of many voxels from a single experiment. The collection of spectroscopic data from multiple adjacent voxels is accomplished by the introduction of phase encoding gradients, which allow the measurement of spectra, for one-dimension, in a slice for two-dimension, and in a volume for three-dimension. Generally, Single Voxel Spectroscopy (SVS) has advantages over MRSI in terms of more explicit spatial localization, more homogeneous shimming, better water suppression,

and shorter acquisition time; however, only one spectrum can be obtained from the acquired SVS data [30]. On the other hand, in MRSI, metabolites are detected from multiple locations and this result is extremely helpful in establishing whether a particular pathological process is localized, bilateral, or diffuse [31]. However, in MRSI, few challenges exist; field inhomogeneity across the tissue under investigation, spectral degradation due to spatial contamination [32] and longer experiment time. MRSI data processing is complicated than SVS data analysis [12]. There are also other problems associated with MRSI experiments specifically at higher field strength known as CSDE (chemical shift displacement error) [33]. In CSDE, proton MRSI signals with different chemical shifts experience different slice.

1.5. MRS data naming convention from different scanners

The output of any MRS experiment contains raw data in time domain and a header file containing all experimental parameters. Raw data from scanners is stored using different names. Hence, it is important to standardize this data-naming pattern for clarity (Fig. 2). There is an urgent need for a universal MRS data portability similar to the Digital Imaging and Communications (DICOM) as available in MRI imaging [34]. DICOM was developed by ACR-NEMA, the American College of Radiology and National Electrical Manufacturers Association for computed axial tomography and MRI images.

2. MRS data analysis

The general schemes for MRS data generation (either in time domain or in k-space for MRSI data) and subsequent data analysis are presented in Fig. 3. MRS data analysis is divided into two stages; preprocessing and quantitation. Preprocessing steps are performed either in the time or frequency domain as pictorially represented in Fig. 3B. Quantitation of metabolites is also performed either in time or frequency domain.

For MRS studies, various experimental conditions impart imperfections to the MRS data. These conditions are: (1) receiver imperfection for not collecting data from the exact start of the FID or from the exact centre of the echo; (2) physiologic motion; (3) fast decaying signals from immobile components; (4) overlapping signals from relatively mobile components; (5) truncation of data before FID has decayed to noise level; and (6) presence of residual water peaks. Hence, acquired MRS data requires preprocessing to minimize error in the quantitation of metabolites.

The preprocessing techniques are different depending on the nature of MRS data processing route (time or frequency domain). Some preprocessing steps can be applied in both domains with similar outcome. There is a direct correspondence between the representative parameters involving FIDs in time domain and metabolite peaks of the spectrum in frequency domain. Hence, quantification of MR signal is performed from both the FID and the spectrum equivalently. Details for preprocessing techniques in time and frequency domains are explained below.

2.1. MRS data analysis in time domain

Time domain MRS data is referred as 'measurement domain' [35–37] as it is a true representation of raw data. Briefly, the time domain signal consists of a mixture of different damped sinusoid signals and these signals are unique and characterized by certain physical parameters (resonance frequency, damping factor, individual phase and amplitude at $t = 0$). The amplitude of the time-domain signal is directly proportional to the number of molecules, the decay constant of the signal characterizes the mobility of the molecules and the frequency of the spectral components

characterizes the identity of the molecules [36]. Accurate and efficient quantitation of MRS signals is accomplished with the help of appropriate model functions. Hence, selection of an appropriate model function is an important step to estimate the intrinsic signal parameters and convert the estimated parameters into biochemical quantities (e.g. metabolite concentrations). Theoretically, the time domain signal can be modeled by a sum of exponentially damped complex sinusoids, where K is assumed to be a known number of expected sinusoids of N time domain data samples as follows [36]:

$$S(t_n)_{n=0,1,\ldots,N-1} = a_0 + \sum_{k=1}^{K} A_k e^{j\Delta\phi_k} e^{(-d_k + j2\pi f_k)t_n} \tag{2}$$

where A_k (amplitude) is proportional to the number of nuclei contributing to the spectral component with frequency f_k and $j = \sqrt{-1}$ and $t_n = t_0 + n\Delta t$ where Δt corresponds to sampling interval. The damping factor d_k provides information about the mobility and macromolecular environment of the nucleus.

The term, $2\pi j f_k t_0$ corresponds to the first-order phase and ϕ_k represents the zero order phase factor. The noise term a_0 is assumed to be circular complex white Gaussian noise [36].

Analysis of time domain data comprises of preprocessing of the MRS data, followed by quantitation of the FIDs using prior knowledge (relations between the spectral components involving amplitudes, damping ratios, frequencies and phases) [38]. The next two sections outline the preprocessing and quantitation methods used in time-domain data analysis.

2.2. Preprocessing in time domain

As indicated earlier, the acquired MRS data is not ideal due to embedded imperfections originating from experimental conditions. Hence, preprocessing of MRS data is required to eliminate certain imperfections. Steps involved in the preprocessing of MRS data in the time domain are as follows:

2.2.1. Eddy current compensation (ECC)
Eddy currents occur due to magnetic field gradients generated during MRS data acquisition. Eddy currents induce time-varying magnetic fields, which in turn cause either frequency-dependent phase shifts, or dephasing (signal loss) of the observed time domain signal. Hence, distortion in signal shape is observed leading to inaccurate spectral quantitation.

The recovery from eddy current corrected signal is accomplished by dividing the water suppressed time domain MRS signal point-wise by the phase part of the unsuppressed water signal [39–42].

2.2.2. Offset correction
The DC (direct current) offset voltage occurs due to the leakage of transmitter reference frequency into the receiver resulting in non-zero mean of free induction decays. Hence, at zero frequency, a spike is generated in the resulting spectrum [43]. The unwanted spike is eliminated during preprocessing period.

2.2.3. Noise filtering
Noise is a time domain random function with certain standard deviation, which is embedded with the acquired signal. It is assumed that in MRS signal, the noise is Gaussian type with zero mean and constant standard deviation. The SNR of MRS signal is correlated with the signal amplitude divided by the standard deviation of the noise. Noise in MRS signal is caused either due to the thermal motion of the charged particles in the sample and/or the thermal motion of the electrons in the coil and receptor paths [44]. Hence, noise reduction is an important objective for SNR
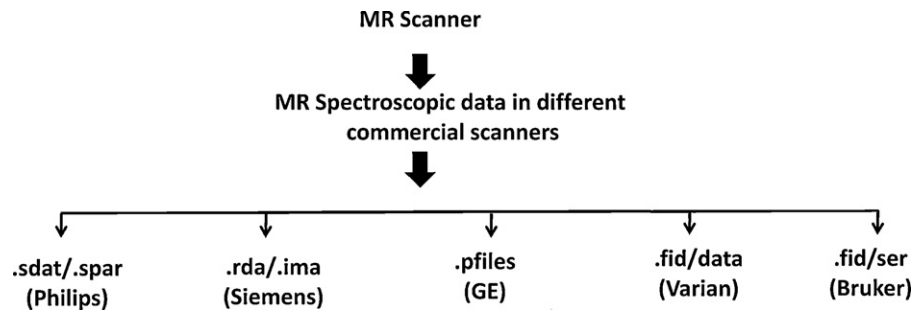
Fig. 2. MRS data naming conventions from different scanners.

improvement. Generally, matched filter is used for noise reduction and the function of such matched filter is similar to pattern of signal decay. For clarity, the matched filter is an exponential decay function with the decay characteristic equal to $T_2{}^*$ of the FID. The selection of the matched filter is not straightforward for multi-compartment FID where compounds have different $T_2{}^*$ values [13,44]. Selection of other filter functions has impact on the line-shape.

2.2.4. Zero filling

Digitized data points in the time domain can be extended with a set of zeros. This implies that part of the signal, which may not have been digitized within the acquisition window, have been fully relaxed and have zero value. The effect of zero filling is to enhance resolution leading to improved spectral visualization only. Data storage space increases depending on the extent of zero filling applied. Zero-filling has a negligible effect for symmetric spin-echo signals [45].

2.2.5. Residual water suppression

Various algorithmic approaches have been applied for the estimation of water component. One strategy is to use low-pass convolution, which suppresses all high frequency components of the spectrum leaving only an estimate of the residual water [46]. Another strategy is to model the water component of the time domain signal as a sum of multiple exponentially damped sinusoids using the HSVD (Hankel Singular Value Decomposition) algorithm [47]. The water signal 'modeled' using either of these techniques is then subtracted from the observed MRS spectrum, leaving only the metabolite signals of interest [48]. The application of digital filter-
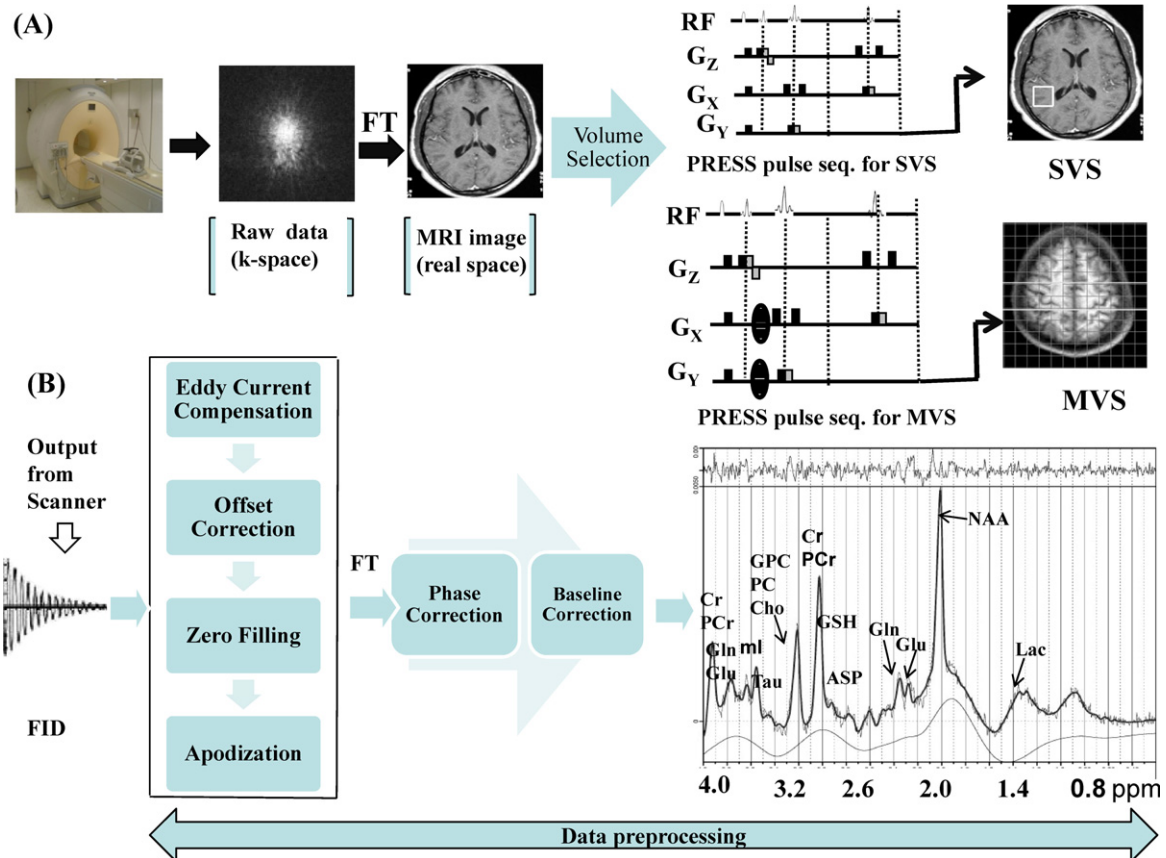

Fig. 3. (A) Diagrammatic representation of MRS data generation and (B) data processing in MRS. SVS and MVS refer to single voxel and multiple voxel spectroscopy. For the sake of simplification, the output from the time domain data is shown as free induction decay (FID) only.

ing on the observed time-domain MRS signal for the elimination of water signal is also available in the literature [49].

2.3. Quantitation of metabolites in time domain

The concentration of the metabolites in a certain localized soft-tissue region is determined by computing the parameters of a certain 'time domain model' function as shown in Eq. (2). In time domain, there are two approaches for the quantitation of metabolites: iterative methods and non-iterative methods [37]. In the iterative methods, typical NLLS (non-linear least squares) methods are used to minimize the difference between the data and the model function using local or global optimization. Another important feature of the iterative methods is the inclusion of prior knowledge (e.g. frequencies, damping factors and phases of some exponentials). One of the early methods of imposing prior knowledge onto the observed signal is the VARPRO (variable projection) method [50]. VARPRO method assumes a Lorentzian line-shape for the individual components of the resonances and fits corresponding decaying exponentials in the time domain, utilizing Osborne's Levenberg–Marquardt local optimization algorithm [51,52]. This iterative methodology in time domain data fitting was further improved by AMARES (Advanced Method for Accurate, Robust and Efficient Spectral)[53,54]. AMARES fitting enables the incorporation of more prior knowledge on the spectral parameters to increase efficiency, convergence rates, overall accuracy, and can also be extended to fit echo signals. AMARES is pre-programmed to switch between Lorentzian, Gaussian or Voigt model line-shape and can be used for fitting spin echoes in addition to FIDs [55]. There are other iterative quantitation methods, such as AQSES (Accurate Quantitation of Short Echo time domain Signals)[56] or QUEST (quantitation based on QUantum ESTimation) which makes use of a metabolite basis set generated from the simulated spectra [57].

Non-iterative methods are either based on the LP (linear prediction) principle or based on the state-space theory like HSVD [58]. Non-iterative methods are less flexible than the iterative methods for the inclusion of prior knowledge, and hence these methods are less suitable for more complicated analysis such as short-echo time MRS signals [37]. In non-iterative methods, model function is confined to only exponential decay and model parameters are chosen in one single step.

Some of the non-iterative methods in time domain include HSVD, HLSVD (Hankel Lanczos Singular Value Decomposition), HTLS (Hankel Total Least Square) and LPSVD (Linear Prediction Singular Value Decomposition).

Finally, model fitting yields the contribution of each input signal. Usually, Cramer–Rao lower bounds (CRLB) provide an estimate for the fitting error or the statistical uncertainty of the metabolic concentration estimate [59].

2.4. MRS data analysis in frequency domain

In frequency domain, processed (Fourier transformed) FID is represented by signals in absorption mode and characterized by their specific resonance frequency, line shape, line width, phase [60]. In an ideal case, free induction decay is considered as a sum of exponentially decaying sinusoid functions. The available model functions for FID in frequency domain consists of Lorentzian $(\exp(-\alpha t))$, Gaussian $(\exp(-\beta t^2))$ and Voigt $(\exp(-\alpha t - \beta t^2))$ line shapes. Mathematically, Fourier transformation is a linear transformation method which decomposes a signal into its constituent frequencies. The information content in the time domain signal $S(t)$ and the frequency domain signal $S(f)$ is the same, provided the acquired signal is "ideal". However, the time domain signals from *in vivo* studies are not "ideal" due to experimental conditions as indicated earlier.

The various preprocessing steps in frequency domain are as follows.

2.4.1. Preprocessing in frequency domain

Certain preprocessing steps (e.g. eddy current compensation, offset correction, apodization) are common to both frequency and time domain, and will not be elaborated in this section. In the frequency-domain, three additional steps namely, phase correction, residual water suppression and baseline correction are applied. Brief description of these preprocessing steps is given below.

2.4.1.1. Phase correction. Certain distortion of the metabolic resonance peak shape can be addressed by phase correction. Phase correction consists of two steps: zero order phase correction and first order phase correction and may be implemented manually or automatically [61]. First, zero order phase correction is implemented, followed by the first-order phase correction. In zero-order phase correction, the same degree of phase correction is implemented for all resonance peaks, while in first-order phase correction, the amount of phase correction effect is dependent on the individual peak [61] under consideration.

2.4.1.2. Baseline correction. This is an important step as inaccurate baseline correction is one of the major sources of variability in quantitation of metabolites. Due to the presence of residual water and/or strong signals arising from lipids, phase corrected spectra are distorted [61]. Baseline can be corrected manually but most of the programs can do it automatically (e.g. LCModel uses spline functions for the baseline).

2.4.1.3. Residual water suppression. Generally, the resonance frequency of water is different compared to other metabolites. Hence filters can be used to remove those specific frequency ranges [62]. One approach is to shift water spectrum to zero frequency using a low pass filter and subsequently subtract it from the original signal. Another approach is to remove the water signal by applying high pass filtering to the FID. In the above two approaches, improper filtering may influence the actual signals of the metabolites which in turn influence the accuracy of quantitation. Special filtering procedures in combination with some other signal treatments have also been proposed [49]. These filters have the ability to remove completely the water spectral line, including its frequency domain tails while minimally affecting those signals which are resonating in the frequency range of the tails.

3. Quantitation of metabolites in frequency domain

Quantitation of metabolites in the frequency domain is accomplished either by peak area integration or by nonlinear least square fitting using model functions. Peak area integration methods works well when peaks in the spectra are well resolved. However, in *in vivo* studies, due to the complexity of the spectra and the overlap of many peaks, quantitation of the spectrum is accomplished by model-based optimization algorithms. These optimization algorithms are based on the regularized nonlinear least squares method [63]. Ideally, the MRS spectrum is a pure "Lorentzian line". But, in reality, MRS signals consist of a mixture of Lorentzian and Gaussian curves or some other distorted shapes. The general equation can be written as [64]

$$S(f) = \sum_{N=1}^{N} A_1 L_N(\nu_{N,f}) + \sum_{N=1}^{N} A_2 G_N(\nu_{N,f}) + \sum_{N=1}^{N} B_N f^N + W(f) \qquad (3)$$

where A_1 and A_2 are the weighted factors for Lorentzian (L_N) and Gaussian contribution (G_N), respectively, and $W(f)$ is a white Gaus-

sian noise [64]. The values of A_1 and A_2 can either be estimated or fixed as prior information. In addition, the third term accounts for possible baseline distortions. A polynomial of order N with coefficient B_N can be used to model the baseline. The estimation of model parameters v_N is obtained by solving a classical non-linear least-square problem.

Several fitting algorithms operating in the frequency domain have been developed in recent years, which allow inclusion of prior knowledge (e.g. amplitude, damping ratios, frequency and phase shifts) as well as relation between spectral components [64,65]. Prior knowledge plays an important role in resolving overlapping peaks or in imposing common line-widths in noisy spectra to improve accuracy of other estimates [64].

4. Fundamental differences in time and frequency domain analysis

There are many differences between time and frequency-domain data analysis. In the time domain method, concentration of a metabolite component is proportional to the amplitude of the signal, whereas in the frequency domain, concentration of metabolites is proportional to the area under the metabolite peak. In time domain method, MRS data is analyzed within the 'measurement domain' [35]. If the measured signal is ideally identified by high SNR, with no truncation and no baseline distortion, then both time and frequency domain methods give the same results within the error limits [66]. Any imperfections in the measured signal, due to experimental conditions (as mentioned earlier) may create a difference in metabolite concentration between the frequency and the time-domain data.

In time-domain data processing, a particular range of good data points can be used for analysis, whereas in the frequency domain, Fourier transformation is performed for all data set and separating the good data points is not possible in frequency domain. In the frequency domain, distortion of the spectrum may arise due to the receiver induced effect at the initial data point as well as due to truncation of the FID [66]. This creates a rolling baseline. Immobile components due to short transverse relaxation time (T_2) generate spectra with broad line widths. These broad lines create a "macromolecular baseline" or a baseline originating from short T_2 components, which makes the baseline approximation more demanding [61].

The time-domain computations can be more memory and time consuming compared to frequency-domain [67]. In general, time-domain methods do not rely on equally spaced sampling intervals, which may be attractive for the multidimensional MRSI techniques [67].

5. MRSI data visualization

There are several methods available for the visualization of processed MRSI data from localized spectra as well as its correlation of spatial distribution of metabolites in various anatomical regions [68–70]. Briefly, a grid is superimposed on the MRI image and corresponding arrays of spectra are plotted, then the spatial distribution of metabolites is overlaid of the corresponding MRI images. In practice, three dimensional MRI (3D volume) and MRSI data are collected from the same subject and data can be viewed at any plane.

5.1. Precision of metabolite quantitation from SVS and MRSI data

In MRSI, the optimization of magnetic field homogeneity over large volumes of tissue is challenging, in contrary, fairly good shimming can be achieved in SVS. There are variations in data quality of different voxels arising from B_0 variations spanning the entire VOI, which causes relative frequency shifts between voxels. This frequency shift correction is required prior to peak fitting of MRSI data.

The variations of B_0 in MRSI data have two major effects: (i) it broadens the signal and sometimes closely space peaks are difficult to resolve and in worst case, peaks are broadened completely and (ii) water peak is over suppressed in some voxels and under suppressed in other voxels pertaining to differences in fitting of the baseline. MRSI data fitting is more complicated compared to SVS and needs much careful attention [71]. The precision of metabolites concentration is more profound in SVS compared to MRSI.

It is important that MRS data (SVS and MRSI) fitting programs provide the Cramer–Rao minimum variance bounds (CRMVBs), which reflect the theoretical standard of precision for the model parameter estimates obtained from the data [72]. The systematic errors (e.g. incorrect prior knowledge) are not included in the parameter estimation. Furthermore, SNR degradation and increase in linewidth, which may lead to systematic errors, are not necessarily reflected in CRMVB estimates [72].

6. Combined approach of frequency domain fitting using time domain models and prior knowledge

Quantification of metabolites is performed mainly by time domain (TD) methods and frequency domain (FD) methods. In TD methods, MRS data is analyze within the 'measurement domain' and has the added advantage for easily handling missing data points and or removing data points at the entry arising from macromolecules. FD methods are suited for frequency selective analysis of time domain MRS data and this can decrease the number of model parameters. Combination of TD and FD methods called TDFD fitting approach has been proposed [73,74]. TDFD approach uses TD models whose parameters are determined by fitting a selected part of the discrete Fourier transform of the TD model involved in that MRS data fitting. Thus TDFD methods can easily handle complex models or the case of missing data as well as frequency selective analysis [35].

7. MRS data processing and quantitation of metabolites using different software packages

Generally, each scanner provides basic MRS data processing software package for quick overview but in most cases, researchers process and analyze MRS data using other software (in-house, freeware or commercial) for more flexibility and in-depth analysis. There is a long list of available MRS data processing software [53,56,75–82]. However, data processing and quantitation using two software packages (LCModel and jMRUI) are mentioned in detail.

8. LCModel

The LCModel is an automatic (non-iterative) commercial software for ^1H MRS data analysis in frequency domain [63] with minimum user input [63]. It is written in C programming language and works in UNIX environment. LCModel is supported by a user-friendly graphical interface, LCMGui. LCMGui automatically calculates the metabolite concentrations and the uncertainties using CR lower bounds formalism [83].

The LCModel [84] analyzes an *in vivo* proton MR spectrum from brain tissue as a linear combination (LC) of 'model' *in vitro* spectra from individual metabolite solutions. These model spectra are supplied along with the software package, or can be generated from *in vitro* model metabolite spectra, which satisfy compatibility requirements with acquisition parameters of the laboratory *in vivo*

data. The LCModel produces the 'best fit' for the analysis of the overlapping peaks [84].

LCModel incorporate maximum "prior information" (e.g. peak position, peak intensity and phase information in the case of multiplets) into the analysis. These prior information do not depends on individual peaks or of related peaks but on the near-complete spectral pattern of each metabolite at a particular magnetic field (1.5 T, 3.0 T, etc.) and type of scanner (Philips, GE, Siemens, etc.). Prior knowledge in frequency domain refers to some of the spectral features, which are consistent with the subjects under study. This prior information is incorporated in a basis set consisting of a separate spectrum for each of the metabolites (e.g. N-acetylaspartate (NAA), creatine, choline, lactate, alanine, myo-inositol, glutamate, scyllo-inositol, glutamine, N-acetyl aspartyl-glutamate (NAAG), aspartate, glucose, GABA and taurine). Inclusion of prior knowledge reduces the number of unknown parameters to be fitted by the LS minimization method and hence, computation time and fitting error are reduced, and the quality of spectral fitting is increased.

The measured brain MR spectrum is compared with a linear combination of spectra from this basis set. The coefficient for each basis function (spectral component) is computed to obtain the best fit to the observed *in vivo* proton MR spectrum. These linear combination coefficients give the maximum-likelihood estimate of the concentration of each metabolite.

The LCModel also optimizes the line-shape of all peaks, their line widths, the frequency shifts, the phase, and the baseline, simultaneously with the linear spectral coefficients. Estimates of uncertainty arising from noise are also presented, using the CR minimum variance bound. The CR bounds represent a lower limit on the statistical errors of the fitted parameters, which are determined by the signal to noise ratio of the spectrum and the mutual interdependence of the model parameters [67].

The major computation time required in the LCModel is to get starting values for the phases for the preliminary analysis and referencing shift for the final analysis. Computation time can be reduced in LCModel analysis if prior information on the approximate phase corrections is included in the "CONTROL file".

The one page output generated using the LCModel program for human data is shown in Fig. 4. The output from the LCModel is available either as a graphic display in a postscript file, or as numerical information in a self-documented text (.table file), or .csv spreadsheet file. The postscript file and the text file contain fitted data and quantitation information of different metabolites, as well as some experimental parameters used in the experiments. The plot in the postscript file contains three thin curves, the middle one is the original data, the one below is the baseline, and the one above is the residual (Fig. 4). The thick curve in red is the LCModel corresponding to the input data. The ppm-range plot of analyzed data is designated as "analysis window". The concentration table in the postscript and the text file provide information about the metabolite concentration ratios. The actual concentrations expressed in millimoles per liter (mmol/L) and the estimated standard deviations are expressed in percent of estimated concentrations. The postscript file indicates the metabolites with acceptable reliability in blue color and the metabolites whose concentrations are significantly lower or higher than normal in red color. In terms of error calculation, the % SD (standard deviation) of estimated concentrations gives the CR lower bound on the estimated concentrations and represent the 95% confidence interval of the estimated concentration values. A percentage standard deviation >50% indicates that the metabolite concentration could range from zero to twice of the estimated concentration. Hence, metabolite concentrations estimated with %SD greater than 50% are considered to be unreliable and the associated metabolites are assumed to be undetectable [85].

The major advantage of the LCModel [84] is that model imperfections due to acquisition effects are included in the acquired basis function and maximum amount of available prior knowledge is used. The disadvantage is that ^{31}P MRS spectral analysis cannot be performed using the LCModel program due to lack of basis set.

Other software packages for MRS data analysis in frequency domain are also available (e.g. MestRe-C/MestRe-Nova (Mestrelab Research) (http://mestrelab.com/), CSX/IMAX Software from Kennedy Krieger Institute, and Johns Hopkins Medicine). Detailed information on CSX/IMAX software is available at http://godzilla.kennedykrieger.org/csx/CSX_IMAX_Jan_2001.pdf.

8.1. Absolute quantitation of metabolites using LCModel

In LCModel, the concentration of the metabolites is calculated using the formula

$$Con_{met} = (Ratio_{area}) \times \frac{2}{N1H_{met}} \times \frac{ATT_{H_2O}}{att_{met}} \times W_{CONC} \qquad (4)$$

where $Ratio_{area}$ refers ratio of the resonance area of metabolite and the resonance area of unsuppressed water. $N1H_{met}$ indicate the number of equivalent protons contributing to the resonance (e.g. $N1H_{met} = 2$ for CH_2 groups). W_{CONC} is the water concentration (in mmol/L) in the voxel, which is 35,880 mmol/L. ATT_{H_2O} and att_{met} are the attenuation factors (generally <1) by which the water and metabolite resonance areas are attenuated by relaxation. Default ATT_{H_2O} value is 0.7.

LCModel performs optimally at short echo and long repetition times. The relaxation time (T_2) corrections to absolute concentrations are only differential, since the T_2 relaxation corrections involve the difference between $1/T_2$ *in vivo* and *in vitro*, but they can still be significant with long TE [63]. The basis set spectra are collected with fully relaxed condition (TR = 10,000 ms) and similar condition in *in vivo* is not feasible due to time constraint. Hence, generally it is assumed that metabolites (*in vivo*) are assumed to be relaxed back with the set repetition time (generally TR 4000 ms) in a clinical setting.
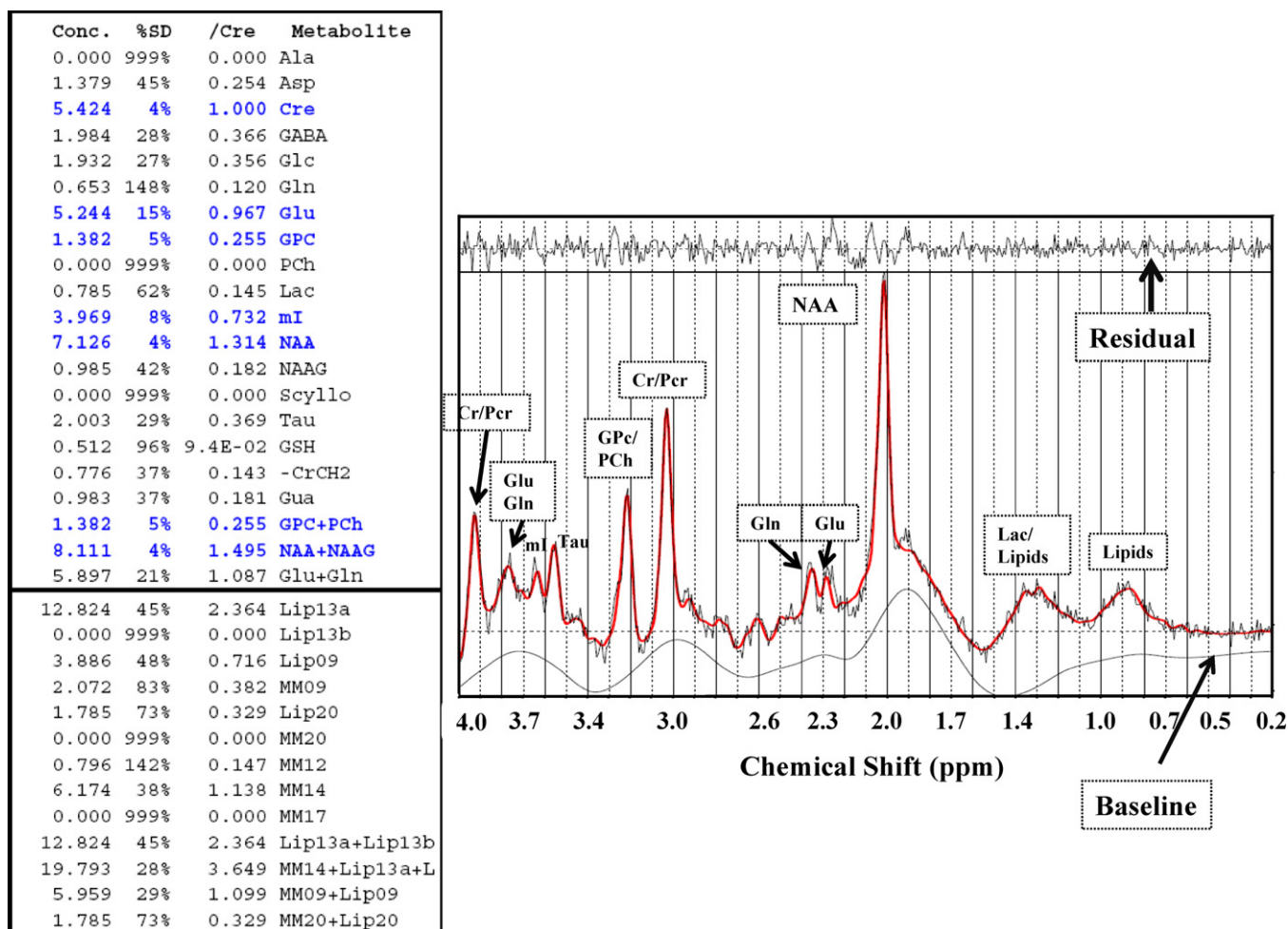
In LCModel, it is also possible to introduce T_1 relaxation time corrections for each metabolite using the correction factor $f_{TR} = (1 - \exp[-TR/T_{1vitro}])/(1 - \exp[-TR/T_{1vivo}])$. Here 'vitro' refers to the relaxation values of the metabolites in the solution [85].

9. jMRUI

jMRUI software uses java-based graphical user interface (GUI) to analyze the time-domain MRS data (FID or echoes) [86] and runs on PCs with Windows, Linux and Unix platforms. Graphical user interface (GUI) in jMRUI is managed by java development kit (JDK), while native code is written in FORTRAN and ANSI C is used for the interface between the GUI and the native code. In comparison to LCModel software, jMRUI requires user interaction [59].jMRUI allows time-domain MRS (^1H and ^{31}P) single voxel as well as in multiple voxel data and can handle large data sets such as time resolved MRS, and MRSI data [59]. Theoretically, signals from metabolites can be computed by quantum mechanics using NMR scope based on the product-operator formalism.

MRS data processing using jMRUI is subdivided into two stages: preprocessing and. quantitation. There are number of preprocessing steps in the time domain. HLSVD filter and HLSVDPro-filter [87] are used for the suppression of water molecules. The time-domain QUALITY deconvolution method helps to remove magnetic field inhomogeneity, contribution to the line-shape yielding Lorenzian line shapes [88]. The Cadzow function is used to filter the signal [54]. jMRUI also uses gabor as a tool for peak extraction and dynamic phase correction. Mathematical operators, like addition, subtraction, multiplication of the signal with a scalar quantity, are

Conc.	%SD	/Cre	Metabolite
0.000	999%	0.000	Ala
1.379	45%	0.254	Asp
5.424	4%	1.000	Cre
1.984	28%	0.366	GABA
1.932	27%	0.356	Glc
0.653	148%	0.120	Gln
5.244	15%	0.967	Glu
1.382	5%	0.255	GPC
0.000	999%	0.000	PCh
0.785	62%	0.145	Lac
3.969	8%	0.732	mI
7.126	4%	1.314	NAA
0.985	42%	0.182	NAAG
0.000	999%	0.000	Scyllo
2.003	29%	0.369	Tau
0.512	96%	9.4E-02	GSH
0.776	37%	0.143	-CrCH2
0.983	37%	0.181	Gua
1.382	5%	0.255	GPC+PCh
8.111	4%	1.495	NAA+NAAG
5.897	21%	1.087	Glu+Gln
12.824	45%	2.364	Lip13a
0.000	999%	0.000	Lip13b
3.886	48%	0.716	Lip09
2.072	83%	0.382	MM09
1.785	73%	0.329	Lip20
0.000	999%	0.000	MM20
0.796	142%	0.147	MM12
6.174	38%	1.138	MM14
0.000	999%	0.000	MM17
12.824	45%	2.364	Lip13a+Lip13b
19.793	28%	3.649	MM14+Lip13a+L
5.959	29%	1.099	MM09+Lip09
1.785	73%	0.329	MM20+Lip20

Fig. 4. Single voxel MRS data was processed by LCModel program. The neurometabolites are assessed and quantifications results are shown separately. Data collected at NBRC using 3T MRI scanner.

available for the normalization of a signal or over a series of signals. It also provides the preprocessing operator to convert an echo signal into an FID signal. All the above operations are performed in time domain except the ER filter and the baseline correction, which are done in frequency domain.

jMRUI software provides for a number of quantitation methods broadly classified as black box methods like Hankel Singular Value Decomposition (HSVD)/Hankel Lanczos Singular Value Decomposition (HLSVD), Hankel Total Least Squeres (HTLS)/Hankel Lanczos Total Least Squares (HLTLS), Linear Predictive Singular Value Decomposition (LPSVD) or interactive methods like VARPRO, AMARES, QUEST and AQSES.

The black box methods are based on either LP (linear prediction) principle or state space formalism. LPSVD method is based on LP principle and uses SVD decomposition to estimate the prediction coefficients in the forward linear prediction procedure expressed as a matrix in a least squares sense. The HSVD/HLSVD and HTLS/HLTLS methods are state space based, where the data is arranged in a Hankel matrix. HSVD computes the Eigen values of the Hankel matrix which are estimates of the signal poles. The HLSVD algorithm is a computationally efficient version of HSVD, which computes only part of the SVD using the Lanczos bidiagonalization algorithm. A variant to the HSVD algorithm is the HTLS algorithm that computes the Total Least Squares (TLS) solution leading to more accurate parameter estimates. HLTLS, like the HLSVD, is a computationally efficient version of HTLS using Lanczos algorithm.

In the interactive quantitation methods the line-widths and concentrations are part of a nonlinear model and are optimized by

fitting the *in vivo* signal with a combination of metabolite signals by nonlinear least squares techniques. The interactive quantification methods in jMRUI are described below.

(1) VARPRO method minimizes the variable projection functional in which the linear and nonlinear parts of the model function are separated. Here the fitting process is separated into one non-linear least squares algorithm in which only the frequencies and the damping factors are optimized, and another linear least squares algorithm in which the amplitudes and phases are fitted. In VARPRO, minimization of the functional is achieved by applying a modified version of the Levenberg–Marquardt algorithm. The advantage of separating fitting process is that no starting values are needed for the linear parameters, and that the number of parameters is halved. VARPRO's capacity to include prior knowledge has made it a reliable tool for accurate and consistent spectral analysis even in challenging data sets with low quality.

(2) AMARES method performs fitting of Lorentzian, Gaussian or Voigt peaks to the signal, with the possibility of including prior knowledge about relations between peaks, such as equal line-widths, or fixed frequency shifts. It minimizes a general functional consisting of the sum of squared differences between the data and the model function. The available biochemical prior knowledge can be expressed as a set of linear relations between parameters resulting in a minimization problem with linear equality constraints. AMARES uses a singlet approach for imposition of prior knowledge. Each of the parameters can be

left unconstrained or kept fixed. In AMARES, a fixed shift or ratio, or a variable shift or ratio, with respect to any unconstrained or fixed parameter of the same type can be imposed. These variable shifts or ratios can then be linked between different groups of peaks. These constraints are substituted in the original functional in order to obtain an unconstrained NLLS optimization problem. AMARES uses a modified version of NL2SOL, a sophisticated NLLS algorithm to minimize the general functional. This algorithm allows the user to specify the upper and lower bounds on the variables. This can be used to impose positive dampings, amplitudes, and upper and lower bounds on frequencies and phases based on the spectral width. AMARES also offers the ability to fit echo signals, an echo being modeled as two FIDs back to back. The left and right parts of the echo are considered to have the same amplitudes, frequencies and phases, but different damping. The damping of the right and left parts can be linked to each other.

(3) QUEST, the most recent method, uses a basis set of metabolite signals that are combined to fit the *in vivo* signal. In this linear combination model, the amplitude/concentration, line-width, phase and frequency shift of each metabolite are considered as free parameters and a nonlinear least square function is minimized with the Levenberg–Marquardt method for nonlinear optimization. All these computations are performed on both the real and imaginary parts of the FID, in the time domain, and not on the frequency domain, as opposed to the LCModel. QUEST can also accommodate a baseline (or background) coming from macromolecules, by truncating a number of points at the FID, fitting the truncated signal with the metabolite basis set, back-extrapolating the estimated model, subtracting it from the *in vivo* signal, and smoothening the result to yield an approximation for the baseline. The metabolite basis set .ml and the peaks file .peak can be generated using NMR scope and used as prior knowledge input for QUEST quantitation method.

MRS data processed using AMARES in jMRUI is presented in Fig. 5. On the top left (Fig. 5) is the information related to the file processed including the number of components asked for and the number of components found. The table gives information about the estimated components: their frequencies, dampings, amplitudes and phases, respectively. CR lower bounds can be used as a measure of the accuracy of the calculation of the amplitude of a certain component.

9.1. Absolute quantitation using jMRUI

The absolute concentration of metabolites from signal intensity as derived by jMRUI can be fitted to a simplified equation as reported [67,89].

$$C_M = \frac{S_M}{S_W} \times C_W \times \frac{n_W}{n_M} \times \frac{f_W^{T_1}}{f_M^{T_1}} \times \frac{f_W^{T_2}}{f_M^{T_2}} \tag{5}$$

where indexes M for metabolite and W for water, C stands for concentration, S for signal intensity, n for the number of chemically equivalent protons, f^{T_1} for spin-lattice relaxation function $(1 - e^{TR/T_1})$, f^{T_2} for spin-spin relaxation function (e^{-TR/T_2}). C_W stands for concentration of water in white matter, which is 35,880 mmol/L same as applied in LCModel.

Mono exponential spin-lattice and spin-spin relaxation are assumed be T_1 (for water: 832 ms; Cho: 1080 ms; Cr: 1240 ms; NAA: 1350 ms) and T_2 (water: 110 ms; Cho: 187 ms; Cr: 156 ms; NAA: 295 ms). The relaxation times of water and respective metabolites measured at 3 T for healthy volunteers were used for relaxation correction [89].

10. Comparative analysis of precision and accuracy of MRS data in LCModel and jMRUI

Comparative analysis of time domain and frequency domain data analysis in prostate [90] and in skeletal muscle [27] are nicely documented. Similar comparative analysis on short echo time brain MRS data is reported [91,92].

In another study, the average metabolite concentrations determined using jMRUI and LCModel from two anatomical regions of Schizophrenic Patients, and the mean CV (coefficient of variance) between scans one week apart are analyzed [92]. MRS data from
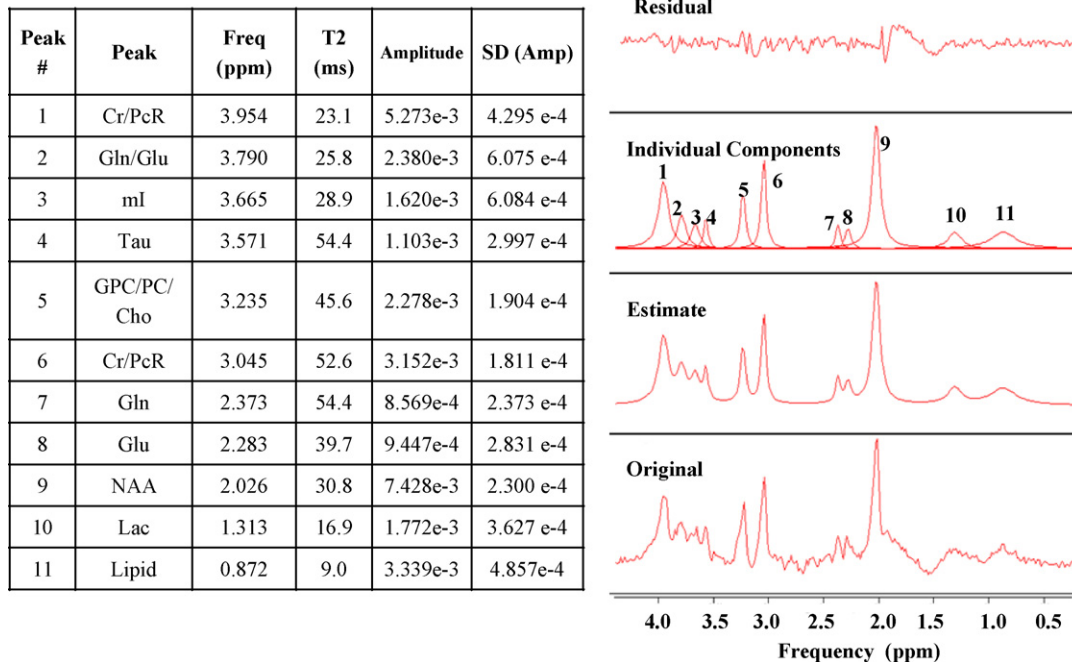

Peak #	Peak	Freq (ppm)	T2 (ms)	Amplitude	SD (Amp)
1	Cr/PcR	3.954	23.1	5.273e-3	4.295 e-4
2	Gln/Glu	3.790	25.8	2.380e-3	6.075 e-4
3	mI	3.665	28.9	1.620e-3	6.084 e-4
4	Tau	3.571	54.4	1.103e-3	2.997 e-4
5	GPC/PC/Cho	3.235	45.6	2.278e-3	1.904 e-4
6	Cr/PcR	3.045	52.6	3.152e-3	1.811 e-4
7	Gln	2.373	54.4	8.569e-4	2.373 e-4
8	Glu	2.283	39.7	9.447e-4	2.831 e-4
9	NAA	2.026	30.8	7.428e-3	2.300 e-4
10	Lac	1.313	16.9	1.772e-3	3.627 e-4
11	Lipid	0.872	9.0	3.339e-3	4.857e-4

Fig. 5. Multiple voxel MRS data processed by jMRUI program. We have used jMRUI (AMARES) package for the quantitation of the metabolites. Data collected at NBRC using 3T MRI scanner.

voxels using PRESS sequence (TE = 40 ms, TR = 2000 ms) were presented for comparative analysis.

There was no significant difference in means between the two scans for any of the metabolites measured (all *P*-values <0.1) [92]. Reproducibility, as measured using the mean CV between scans, for the frontal voxel (within patient) was excellent (e.g. NAA from LCModel: 2%; MRUI: 4%, Cho from LCModel: 2%; MRUI: 2%, creatine from LCModel: 3%; MRUI: 4% and mI from LCModel: 13%; MRUI: 7%) [92].

Another comparative analysis using LCModel and jMRUI (AMARES) of ^{1}H MRS data (short echo time) for the quantification of metabolites on human brain was reported [91]. It was reported that the inclusion of macromolecules and lipids basis set in LCModel improves the accuracy of the results compared to the spline fit of the baseline. Similar observation with jMRUI is that the inclusion of macromolecules and lipids in the prior knowledge improves the precision and accuracy of the metabolites (NAA, Cho, creatine and mI) quantitation significantly.

The concentration of the metabolites (NAA, Cho, creatine and mI) shows slight overestimation in LCModel, whereas, jMRUI generates slightly underestimated concentrations of those metabolites. Glx concentration was definitely more precise and accurately determined by LCModel than jMRUI in this study. In both methods, the metabolite-to-creatine ratios show that the metabolites, NAA, Cho and mI have same general trend [91]. LCModel analysis was superior to jMRUI (AMARES) for determining Glx/Cr ratios in that study [91].

In the same study, for the absolute quantitation of macromolecules (abbreviated as mm1, mm2, mm3, mm4, mm5, mm6 and mm7), both LCModel and jMRUI exhibit poor accuracy and very low precision, except for mm1 and mm2 using jMRUI, and mm2 using LCModel fitting. The same study, also reports 10–20% underestimation of the lipid concentrations using LCModel analysis, but high SD (standard deviation) discourages the acceptance of the value for any practical relevance. On contrary, jMRUI (AMARES) analysis exhibits poor accuracy and very low precision for lipid concentration determination [91].

11. Selection of appropriate prior knowledge involving macromolecules and lipid resonances

Due to inherent immobility, peaks originating from macromolecules (e.g. cytosolic proteins) and lipids are broad (characterized by short T_2). These broad peaks distort the baseline and subsequently cause a major source of variability in fitting MRS data absolute quantification. It is important that macromolecular content in the *in vivo* spectra cannot be analyzed using simple model function as various types of macromolecules essentially contribute to this "gross" spectrum [93].

In the frequency domain (i.e. LCModel), the estimation of macromolecule using mathematical approaches is done by sum of splines. In the time domain (jMRUI), it is accomplished by weighting the first 20 points in AMARES and by Subtract approach in QUEST. The Subtract-QUEST method (jMRUI) is based on a semi-parametric approach. It untangles the background from the metabolite signal, models it separately and fits the untangled metabolite signal using a parametric nonlinear least-squares approach sequentially.

An advantage of the mathematical approaches is the time saving, because we do not need to acquire the spectrum of macromolecules separately.

However, more prior knowledge (which cannot be obtained by mathematical estimation) on the macromolecule signal is needed to obtain an accurate estimation of the metabolite concentrations at higher magnetic field, where the macromolecule spectrum is better resolved. This prior knowledge we are usually obtaining by

measuring the macromolecule signal *in vivo* by inversion recovery. The quantification of macromolecules and lipids is an area of active research [94–96].

In LCModel, the addition of macromolecular and lipid basis set improves significantly precision and accuracy of the neurometabolites [91]. Similarly, in case of jMRUI (AMARES), inclusion of background in the prior knowledge adds much improvement in the precision and accuracy of the neurometabolites.

12. Criteria for choosing MRS software package for data processing

Although two MRS data processing software packages are discussed in this manuscript, there are many other MRS data processing software packages used in different laboratories. The consideration for MRS data software should be based on few factors. These factors include software capabilities (i.e. SVS or MRS data analysis); automation; flexibility for changing analysis for new pulse sequences, performance, cross-platform compatibility, and user friendliness, as well as in-depth documentation, nuclei of interest (^{1}H MRS or ^{31}P MRS) and availability (free for academic use or commercial). The author has refrained from selecting a particular software package, but certainly, the criteria for choosing appropriate software as mentioned above will help the user.

13. Conclusions

Preprocessing of *in vivo* MRS data is crucial for the enhancement of the measured signal which has a great significance in clinical studies. We have presented the details of MRS data processing both in time and frequency domains in a sequential manner. Two MRS data processing software packages are discussed with inherent mathematical approach. A comparative analysis of signal processing in time and frequency domain is performed. Data quality using LCModel and jMRUI is presented specifically focusing on precision and accuracy. MRS data (Figs. 4 and 5) was collected with the approval of the institutional human ethics committee using 3 T MRI scanner at NBRC.

Conflict of interest

There is no conflict of interest in this work.

Acknowledgements

References

[1] Mandal PK, Majumdar A. A comprehensive discussion of HSQC and HMQC pulse sequences. Concepts Magn Reson A 2004;20A:1–23.

[2] Mandal PK, Simplaceanu V, Fodale V. Intravenous anesthetic diazepam does not induce amyloid-beta peptide oligomerization but diazepam co-administered with halothane oligomerizes amyloid-beta peptide: an NMR study. J Alzheimers Dis 2010;20:127–34.

[3] Mandal PK, Bhavesh NS, Chauhan VS, Fodale V. NMR investigations of amyloid-beta peptide interactions with propofol at clinically relevant concentrations with and without aqueous halothane solution. J Alzheimers Dis 2010;21:1303–9.

[4] Kreis R, Hofmann L, Kuhlmann B, Boesch C, Bossi E, Huppi PS. Brain metabolite composition during early human brain development as measured by quantitative in vivo 1H magnetic resonance spectroscopy. Magn Reson Med 2002;48:949–58.

[5] Kreis R. 1HMR spectroscopy outside the brain. MAGMA 2002:1512–7.

[6] Mandal PK. Magnetic Resonance Spectroscopy (MRS) and its application in Alzheimer's disease. Concepts Magn Reson A: Bridging Educ Res 2007;30:40–64.

[7] Frahm J, Bruhn H, Gyngell ML, Merboldt KD, Hanicke W, Sauter R. Localized proton NMR spectroscopy in different regions of the human brain in vivo. Relaxation times and concentrations of cerebral metabolites. Magn Reson Med 1989;11:47–63.

[8] Bachert P, Bellemann ME, Layer G, Koch T, Semmler W, Lorenz WJ. In vivo 1H, 31P-[1H] and 13C-[1H] magnetic resonance spectroscopy of malignant histiocytoma and skeletal muscle tissue in man. NMR Biomed 1992;5:161–70.

[9] Gruetter R, Adriany G, Merkle H, Andersen PM. Broadband decoupled, 1H-localized 13C MRS of the human brain at 4 Tesla. Magn Reson Med 1996;36:659–64.

[10] Sanchez V, Redfield AG, Johnston PD, Tropp J. Nuclear Overhauser effect in specifically deuterated macromolecules: NMR assay for unusual base pairing in transfer RNA. Proc Natl Acad Sci USA 1980;77:5659–62.

[11] Barker PB, Bizzi A, Stefano ND, Gullapalli RP, Lin DDM. Clinical MR spectroscopy: techniques and applications. Cambridge University Press; 2010.

[12] de Graaf RA. In vivo NMR spectroscopy – 2nd edition: principles and techniques. John Wiley & Sons; 2007. p. 1–592.

[13] Ernst RR, Bodenhausen G, Wokaun A. Principles of nuclear magnetic resonance in one and two dimensions. Oxford University Press; 1990.

[14] Satlin A, Bodick N, Offen WW, Renshaw PF. Brain proton magnetic resonance spectroscopy (1H-MRS) in Alzheimer's disease: changes after treatment with xanomeline, an M1 selective cholinergic agonist. Am J Psychiatry 1997;154:1459–61.

[15] Parnetti L, Tarducci R, Presciutti O, et al. Proton magnetic resonance spectroscopy can differentiate Alzheimer's disease from normal aging. Mech Ageing Dev 1997;97:9–14.

[16] Rango M, Arighi A, Biondetti P, et al. Magnetic resonance spectroscopy in Parkinson's disease and parkinsonian syndromes. Funct Neurol 2007;22:75–9.

[17] Federico F, Simone IL, Lucivero V, et al. Proton magnetic resonance spectroscopy in Parkinson's disease and progressive supranuclear palsy. J Neurol Neurosurg Psychiatry 1997;62:239–42.

[18] Atmaca M, Yildirim H, Ozdemir H, Poyraz AK, Tezcan E, Ogur E. Hippocampal 1H MRS in first-episode bipolar I patients. Prog Neuropsychopharmacol Biol Psychiatry 2006;30:1235–9.

[19] Kato T, Takahashi S, Inubushi T. Brain lithium concentration by 7Li- and 1H-magnetic resonance spectroscopy in bipolar disorder. Psychiatry Res 1992;45:53–63.

[20] Bartha R, al-Semaan YM, Williamson PC, et al. A short echo proton magnetic resonance spectroscopy study of the left mesial-temporal lobe in first-onset schizophrenic patients. Biol Psychiatry 1999;45:1403–11.

[21] Nasrallah HA, Skinner TE, Schmalbrock P, Robitaille PM. Proton magnetic resonance spectroscopy (1H MRS) of the hippocampal formation in schizophrenia: a pilot study. Br J Psychiatry 1994;165:481–5.

[22] Grande S, Giovannini C, Guidoni L, et al. 1H MRS signals from glutathione may act as predictive markers of apoptosis in irradiated tumour cells. Radiat Prot Dosimetry 2006;122:205–6.

[23] Sijens PE, Levendag PC, Vecht CJ, van Dijk P, Oudkerk M. 1H MR spectroscopy detection of lipids and lactate in metastatic brain tumors. NMR Biomed 1996;9:65–71.

[24] Longo R, Pollesello P, Ricci C, et al. Proton MR spectroscopy in quantitative in vivo determination of fat content in human liver steatosis. J Magn Reson Imaging 1995;5:281–5.

[25] Lowry M, Liney GP, Turnbull LW, Manton DJ, Blackband SJ, Horsman A. Quantification of citrate concentration in the prostate by proton magnetic resonance spectroscopy: zonal and age-related differences. Magn Reson Med 1996;36:352–8.

[26] Hu J, Willcott MR, Moore GJ. Two-dimensional proton chemical-shift imaging of human muscle metabolites. J Magn Reson 1997;126:187–92.

[27] Weis J, Johansson L, Ortiz-Nieto F, Ahlstrom H. Assessment of lipids in skeletal muscle by LCModel and AMARES. J Magn Reson Imaging 2009;30:1124–9.

[28] Van Zijl PC, Barker PB. Magnetic resonance spectroscopy and spectroscopic imaging for the study of brain metabolism. Ann N Y Acad Sci 1997;820:75–96.

[29] Barker PB, Lin DDM. In vivo proton MR spectroscopy of the human brain. Prog Nucl Magn Reson Spectrosc 2006;49:99–128.

[30] Hsu YY, Chang C, Chang CN, Chu NS, Lim KE, Hsu JC. Proton MR spectroscopy in patients with complex partial seizures: single-voxel spectroscopy versus chemical-shift imaging. Am J Neuroradiol 1999;20:643–51.

[31] Constans JM, Meyerhoff DJ, Norman D, Fein G, Weiner MW. 1H and 31p magnetic resonance spectroscopic imaging of white matter signal hyperintensity areas in elderly subjects. Neuroradiology 2005;37:615–23.

[32] Van Au Duong M, Audoin B, Le Fur Y, et al. Relationships between gray matter metabolic abnormalities and white matter inflammation in patients at the very early stage of MS: a MRSI study. J Neurol 2007;254:914–23.

[33] Scheenen TW, Klomp DW, Wijnen JP, Heerschap A. Short echo time 1H-MRSI of the human brain at 3 T with minimal chemical shift displacement errors using adiabatic refocusing pulses. Magn Reson Med 2008;59:1–6.

[34] Rosslyn V. National electrical manufacturers' association. Digital Imaging and Communications in Medicine (DICOM). NEMA; 1996.

[35] Elster C, Link A, Schubert F, Seifert F, Walzel M, Rinneberg H. Quantitative MRS: comparison of time domain and time domain frequency domain methods using a novel test procedure. Magn Reson Imaging 2000;18:597–606.

[36] Vanhamme L, Sundin T, Van Hecke P, Van Huffel S. MR spectroscopy quantitation: a review of time-domain methods. NMR Biomed 2001;14:233–46.

[37] Poullet JB, Sima DM, Van Huffel S. MRS signal quantitation: a review of time- and frequency-domain methods. J Magn Reson 2008;195:134–44.

[38] Kreis R, Ernst T, Ross BD. Development of the human brain: in vivo quantification of metabolite and water content with proton magnetic resonance spectroscopy. Magn Reson Med 1993;30:424–37.

[39] van der Graaf M. In vivo magnetic resonance spectroscopy: basic methodology and clinical applications. Eur Biophys J 2010;39:527–40.

[40] Klose U. In vivo proton spectroscopy in presence of eddy currents. Magn Reson Med 1990;14:26–30.

[41] Knight-Scott J. Application of multiple inversion recovery for suppression of macromolecule resonances in short echo time (1)H NMR spectroscopy of human brain. J Magn Reson 1999;140:228–34.

[42] Bartha R, Drost DJ, Menon RS, Williamson PC. Spectroscopic lineshape correction by QUECC: combined QUALITY deconvolution and eddy current correction. Magn Reson Med 2000;44:641–5.

[43] Salibi N, Brown MA. Clinical MR spectroscopy: first principles. Wiley-Liss, Inc; 1998. p. 106–12.

[44] Jiru F. Introduction to post-processing techniques. Eur J Radiol 2008;67:202–17.

[45] Ebel A, Dreher W, Leibfritz D. Effects of zero-filling and apodization on spectral integrals in discrete Fourier-transform spectroscopy of noisy data. J Magn Reson 2006;182:330–8.

[46] Marion D, Ikura K, Bax A. Improved solvent suppression in one- and two-dimensional NMR spectra by convolution of time domain data. J Magn Reson 1989;84:425–30.

[47] Van der Boogart A, Van Ormondt D, Pijnappel WW, De Beer R, Ala-Korpela A. Removal of the water resonance from 31P magnetic resonance spectra. J Magn Reson 1991;91:175–95.

[48] Vanhamme L, Fierro RD, Van Huffel S, de Beer R. Fast removal of residual water in proton spectra. J Magn Reson 1998;132:197–203.

[49] Sundin T, Vanhamme L, Van Hecke P, Dologlou I, Van Huffel S. Accurate quantification of (1)H spectra: from finite impulse response filter design for solvent suppression to parameter estimation. J Magn Reson 1999;139:189–204.

[50] van der Veen JW, de Beer R, Luyten PR, van Ormondt D. Accurate quantification of in vivo 31P NMR signals using the variable projection method and prior knowledge. Magn Reson Med 1988;6:92–8.

[51] Stubbs M, Van den Boogaart A, Bashford CL, et al. 31P-magnetic resonance spectroscopy studies of nucleated and non-nucleated erythrocytes; time domain data analysis (VARPRO) incorporating prior knowledge can give information on the binding of ADP. Biochim Biophys Acta 1996;1291:143–8.

[52] Osborne MR. Numerical methods for non-linear optimization. London: Academic Press; 1972.

[53] Vanhamme L, van den Boogaart A, Van Huffel S. Improved method for accurate and efficient quantification of MRS data with use of prior knowledge. J Magn Reson 1997;129:35–43.

[54] Naressi A, Couturier C, Devos JM, et al. Java-based graphical user interface for the MRUI quantitation package. Magn Reson Mater Phys Biol Med 2001;12:141–52.

[55] van den Boogaart A. Quantitative data analysis of in vivo MRS data sets. Magn Reson Chem 1997;35:S146–52.

[56] Poullet JB, Sima DM, Simonetti AW, et al. An automated quantitation of short echo time MRS spectra in an open source software environment: AQSES. NMR Biomed 2007;20:493–504.

[57] Ratiney H, Sdika M, Coenradie Y, Cavassila S, van Ormondt D, Graveron-Demilly D. Time-domain semi-parametric estimation based on a metabolite basis set. NMR Biomed 2005;18:1–13.

[58] Barkhuijsen H, de Beer R, Bovee WM, Creyghton JH, van Ormondt D. Application of linear prediction and singular value decomposition (LPSVD) to determine NMR frequencies and intensities from the FID. Magn Reson Med 1985;2:86–9.

[59] Helms G. The principles of quantification applied to in vivo proton MR spectroscopy. Eur J Radiol 2008;67:218–29.

[60] Zandt HJAI, van der Graaf M, Heerschap A. Common processing of in vivo MR spectra. NMR Biomed 2001;14:224–32.

[61] Ernst T, Linda C. Data processing and interpretation ISMER; 2006.

[62] Coron A, Vanhamme L, Antoine JP, Van Hecke P, Van Huffel S. The filtering approach to solvent peak suppression in MRS: a critical review. J Magn Reson 2001;152:26–40.

[63] Provencher SW. Automatic quantitation of localized in vivo H-1 spectra with LCModel. NMR Biomed 2001;14:260–4.

[64] Landini L, Postitano V, Santarelli MF. Advanced image processing in magnetic resonance imaging. CRS Press, Taylor and Francis; 2005. p. 418–421.

[65] de Graaf AA, Bovee WM. Improved quantification of in vivo 1H NMR spectra by optimization of signal acquisition and processing and by incorporation of prior knowledge into the spectral fitting. Magn Reson Med 1990;15:305–19.

[66] Vandenboogaart A, Alakorpela M, Jokisaari J, Griffiths JR. Time and frequency-domain analysis of NMR data compared – an application to 1d H-1 spectra of lipoproteins. Magn Reson Med 1994;31:347–58.

[67] Kreis R. Quantitative localized 1H MR spectroscopy for clinical use. Prog Nucl Magn Reson Spectrosc 1997;31:155–95.

[68] Maudsley AA, Hilal SK, Simon HE, Wittekoek S. In vivo MR spectroscopic imaging with P-31. Work in progress. Radiology 1984;153:745–50.

[69] Vigneron DB, Nelson SJ, Murphy-Boesch J, et al. Chemical shift imaging of human brain: axial, sagittal, and coronal P-31 metabolite images. Radiology 1990;177:643–9.

[70] Swanson MG, Noworotski SM, Kurhanewicz J. Magnetic resonance spectroscopy and spectroscopic imaging of the prostate, breast, and liver. In: Webb GA, editor. Modern Magnetic Resonance. 2006. p. 1099–111.

[71] McLean MA. 1D and 2D quantification methods in the international society for magnetic resonance; 2006.

[72] Jansen JFA, Backes WH, Nicolay K, Kooi ME. 1H MR spectroscopy of the brain: absolute quantification of metabolites. Radiology 2006;240:318–32.

[73] Soher BJ, Young K, Govindaraju V, Maudsley AA. Automated spectral analysis III: application to in vivo proton MR spectroscopy and spectroscopic imaging. Magn Reson Med 1998;40:822–31.

[74] Slotboom J, Boesch C, Kreis R. Versatile frequency domain fitting using time domain models and prior knowledge. Magn Reson Med 1998;39:899–911.

[75] Maudsley AA, Wu Z, Meyerhoff DJ, Weiner MW. Automated processing for proton spectroscopic imaging using water reference deconvolution. Magn Reson Med 1994;31:589–95.

[76] Bhat H, Sajja BR, Narayana PA. Fast quantification of proton magnetic resonance spectroscopic imaging with artificial neural networks. J Magn Reson 2006;183:110–22.

[77] De Neuter B, Luts J, Vanhamme L, Lemmerling P, Van Huffel S. Java-based framework for processing and displaying short-echo-time magnetic resonance spectroscopy signals. Comput Methods Programs Biomed 2007;85:129–37.

[78] Bartha R, Drost DJ, Williamson PC. Factors affecting the quantification of short echo in-vivo 1H MR spectra: prior knowledge, peak elimination, and filtering. NMR Biomed 1999;12:205–16.

[79] Shic F, Ross B. Automated data processing of [1H-decoupled] 13C MR spectra acquired from human brain in vivo. J Magn Reson 2003;162:259–68.

[80] Mierisova S, van den Boogaart A, Tkac I, Van Hecke P, Vanhamme L, Liptaj T. New approach for quantitation of short echo time in vivo 1H MR spectra of brain using AMARES. NMR Biomed 1998;11:32–9.

[81] Maudsley AA, Darkazanli A, Alger JR, et al. Comprehensive processing, display and analysis for in vivo MR spectroscopic imaging. NMR Biomed 2006;19:492–503.

[82] Soher BJ, Young K, Bernstein A, Aygula Z, Maudsley AA. GAVA: spectral simulation for in vivo MRS applications. J Magn Reson 2007;185:291–9.

[83] Provencher SW. Automatic quantitation of localized in vivo 1H spectra with LCModel. NMR Biomed 2001;14:260–4.

[84] Provencher SW. Estimation of metabolite concentrations from localized in vivo proton NMR spectra. Magn Reson Med 1993;30:672–9.

[85] Srinivasan R, Sailasuta N, Hurd R, Nelson S, Pelletier D. Evidence of elevated glutamate in multiple sclerosis using magnetic resonance spectroscopy at 3 T. Brain 2005;128:1016–25.

[86] Naressi A, Couturier C, Castang I, de Beer R, Graveron-Demilly D. Java-based graphical user interface for MRUI, a software package for quantitation of in vivo/medical magnetic resonance spectroscopy signals. Comput Biol Med 2001;31:269–86.

[87] Pijnappel WW, de Beer R, van den Boogaart A, van Ormondt D. SVD-based quantification of magnetic resonance signals. J Magn Reson 1992;97:122–34.

[88] de Graaf AA, van Dijk JE, Bovee WM. QUALITY: quantification improvement by converting lineshapes to the Lorentzian type. Magn Reson Med 1990;13:343–57.

[89] Aboul-Enein F, Krssak M, Hoftberger R, Prayer D, Kristoferitsch W. Reduced NAA-levels in the NAWM of patients with MS is a feature of progression. A study with quantitative magnetic resonance spectroscopy at 3 Tesla. PLoS ONE 2010;5:e11625.

[90] Pels P, Ozturk-Isik E, Swanson MG, et al. Quantification of prostate MRSI data by model-based time domain fitting and frequency domain analysis. NMR Biomed 2006;19:188–97.

[91] Kanowski M, Kaufmann J, Braun J, Bernarding J, Tempelmann C. Quantitation of simulated short echo time 1H human brain spectra by LCModel and AMARES. Magn Reson Med 2004;51:904–12.

[92] Mullins PG, Rowland L, Bustillo J, Bedrick EJ, Lauriello J, Brooks WM. Reproducibility of 1H-MRS measurements in schizophrenic patients. Magn Reson Med 2003;50:704–7.

[93] Seeger U, Klose U, Mader I, Grodd W, Nagele T. Parameterized evaluation of macromolecules and lipids in proton MR spectroscopy of brain diseases. Magn Reson Med 2003;49:19–28.

[94] Ratiney H, Coenradie Y, Cavassila S, van Ormondt D, Graveron-Demilly D. Time-domain quantitation of 1H short echo-time signals: background accommodation. Magma 2004;16:284–96.

[95] Cudalbu C, Mlynarik V, Xin L, Gruetter R. Comparison of T_1 relaxation times of the neurochemical profile in rat brain at 9.4 tesla and 14.1 tesla. Magn Reson Med 2009;62:862–7.

[96] Kassem MN, Bartha R. Quantitative proton short-echo-time LASER spectroscopy of normal human white matter and hippocampus at 4 Tesla incorporating macromolecule subtraction. Magn Reson Med 2003;49:918–27.